Epoxy−Clay Fabric Film Composites with Unprecedented Oxygen-Barrier Properties

Kostas S. Triantafyllidis,† Peter C. LeBaron, In Park, and Thomas J. Pinnavaia*

Department of Chemistry, Michigan State University, East Lansing, Michigan 48824

Received April 9, 2006. Revised Manuscript Received June 28, 2006

A new barrier-film chemistry is described in which two materials, namely a clay fabric film and a polymer, are combined to form a composite with gas-barrier properties that are far superior to those of the parent end members. Homoionic inorganic smectite clay fabric films of sodium montmorillonite and synthetic lithium fluorohectorite were cast in self-supported film form, impregnated with liquid epoxy resin and amine curing agent, and then cured to form the final epoxy−clay fabric film composite. The oxygen permeabilities of the epoxy−clay fabric film composites were lower by 2−3 orders of magnitude in comparison to that of the pristine polymer and by 3−4 orders of magnitude in comparison to that of the pristine clay film. This unprecedented reduction in oxygen permeability was attributed in part to the high volume fraction (∼77%) of highly aligned and nonswellable clay nanolayers in the fabric film and to the polymer filling of voids formed between imperfectly tiled clay platelet edges in the film. Mixed organic−inorganic ion-exchange forms of clay fabric films made through ion-exchange reactions of inorganic clay films form a heterostructure in which the outer regions of the film contain a swellable organoclay phase and the interior regions retain the nonswellable inorganic clay barrier phase. The modulus and glass-transition temperature of the polymer phase is not compromised upon formation of the clay fabric film composites.

Introduction

The reduction of gas permeability of polymers and plastics to small molecules is an important need for a vast number of applications, such as food and beverage packaging, liquid hydrogen storage and transportation, moisture- and air-proof coatings, etc. A common approach to achieving a low permeability in an engineering polymer is to sandwich a nonengineering polymer with good barrier properties (e.g., polyethylene−poly(vinyl alcohol) copolymer, EVOH) between sheets of an engineering polymer with good strength but poor barrier properties (e.g., high-density polyethylene, HDPE).[1] However, for many applications, the marriage between barrier polymers and engineering polymers does not provide the desired level of barrier performance. Consequently, there have been many efforts to improve the chemistry of barrier films.[2−9]

Organic−inorganic hybrid nanocomposites comprise a relatively new class of polymeric materials with improved properties.[10−19] The organic component usually comprises a thermoset or thermoplatic polymer, whereas the inorganic component is a layered silicate material, such as smectite clay, a layered silicic acid, layered double hydroxides, or a similar nanoparticle phase. The improvement in the properties of the nanocomposites compared to the pristine polymers is attributed mainly to the unique phase morphology and the interfacial properties provided by the highly dispersed nanoscale inorganic component. Consequently, loadings of only ∼5 wt % exfoliated silicate nanoparticles in polymer−clay nanocomposite materials, for example, result in significant enhancement in properties. A wide variety of other layered materials are potentially well-suited for the formation of organic−inorganic nanocomposites, because their lamellar elements have high in-plane strength and stiffness and a high aspect ratio. However, the smectite clays[20] (e.g., montmorillonite, hectorite) and related layered silicates are the

* Corresponding author. E-mail: pinnavaia@chemistry.msu.edu.
† Present address: Department of Chemistry, Aristotle University of Thessaloniki, 54124 Thessaloniki, Greece

(1) Matayabas, J. C., Jr.; Turner, S. R. In *Polymer−Clay Nanocomposites*; Pinnavaia, T. J., Beall, G. W., Eds.; John Wiley & Sons: New York, 2000; p 207.
(2) Barbee, R. B.; Gilmer, J. W.; Matayabas, J. C., Jr.; Lan, T.; Psihogios, V. PCT Int. Appl. 34376, 2000.
(3) Chu, S.-C.; Keung, J. K.; Su, T.-K. PCT Int. Appl. 40404, 2000.
(4) Barsotti, R. J.; Winter, D. J., PCT Int. Appl. 49072, 2000.
(5) Sakatani, Y.; Kuroda, T.; Okino, O. Jpn. Pat. 10086268, 1998.
(6) Elspass, C. W.; Kresge, E. N.; Peiffer, D. G.; Hseih, D.-T.; Chludzinski, J. J. PCT Int. Appl. 9700910, 1997.
(7) Kotani, K.; Kawakita, T.; Sakaya, T.; Kuroda, T. Can. Pat. Appl. 2101037, 1994.
(8) Mueller, C.; Kaas, R.; Fillon, B.; Tournier, S.; Lerda, J.-J. PCT Int. Appl. 187566, 2001.
(9) Bernard, L. G.; Clauberg, H.; Cyr, M. J.; Gilmer, J. W.; Matayabas, J. C., Jr.; Owens, J. T.; Stewart, M. E.; Turner, S. R.; Bagrodia, S. PCT Int. Appl. 110945, 2001.
(10) Vaia, R. A.; Giannelis, E. P. *MRS Bull.* **2001**, *26*, 394.
(11) Pinnavaia, T. J., Beall, G. W., Eds. *Polymer−Clay Nanocomposites*; Jonh Wiley & Sons: New York, 2000.
(12) LeBaron, P. C.; Wang, Z.; Pinnavaia, T. J. *Appl. Clay Sci.* **1999**, *15*, 11.
(13) Lagaly, G. *Appl. Clay Sci.* **1999**, *15*, 1.
(14) Giannelis, E. P. *Adv. Mater.* **1996**, *8*, 29.
(15) Manias, E.; Touny, A.; Wu, L.; Strawhecker, K.; Lu, B.; Chung, T. C. *Chem. Mater.* **2001**, *13*, 3516.
(16) Mark, J. E. *Mater. Res. Soc. Symp. Proc.* **2001**, *661*, KK1.1/1.
(17) Fukushima, H.; Drzal, L. T. *Proc. Annu. Meet. Adhes. Soc.* **2000**, *23rd*, 189.
(18) Drzal, L. T.; Sugiura, N.; Hook, D. *Compos. Interfaces* **1997**, *4*, 337.
(19) Petrovicova, E.; Knight, R.; Schadler, L. S.; Twardowski, T. E. *J. Appl. Polym. Sci.* **2000**, *78*, 2272.
(20) Pinnavaia, T. J. *Science* **1983**, *220*, 365.

10.1021/cm060825t CCC: $33.50
Published on Web 08/04/2006

materials of choice for polymer nanocomposite design, [21−23] mainly because of their rich intercalation and ion-exchange chemistry, which allows them to be chemically modified and made compatible with the polymer matrix.

The barrier properties of the polymer−clay nanocomposites have attracted the interest of the packaging and coatings industry, and several studies have focused on developing new high-barrier nanocomposite materials. [1,19,24−34] The gas permeability of a typical composite containing 1−5 wt % clay could be reduced to 2−6-fold, depending on the degree to which the clay nanolayers have been dispersed and oriented in the polymer matrix. Recent studies[35] on the structural and barrier properties of olefinic nanocomposites have shown the importance of the interfacial properties between the polymer and the organoclay surface. An oxygen-barrier improvement as high as 300-fold was observed for wax/LDPE−organoclay nanocomposites, provided that the surface of the organoclay was appropriately modified with poly(ethylene glycol)-based copolymers. Also, it was found that large differences between the melting points of polyolefin systems (such as LDPE alone) and organic modifiers result in significant decreases in barrier enhancement because of phase separation that occurs upon recrystallization of the polymer in the presence of an organoclay modifier that remains in the liquid state.

In the present work, we report highly impermeable polymer−clay composites formed by impregnating free-standing clay fabric films with polymer. The polymer used in this study was a thermoset epoxy resin, of the type used for the fabrication of lightweight gas-storage containers and aerospace components. The oxygen permeabilities measured for the different epoxy−clay film composites were 2−3 orders of magnitude lower than that of the pristine polymer itself.

Experimental Section

Materials. The epoxide resin was a diglycidyl ether of bisphenol A (DGEBA), more specifically, Shell EPON 826 with an epoxy equivalent weight of ∼182 g/equivalent.

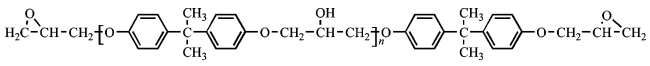

$n = 0$ (90 %), 1 (10 %)

The curing agent was a polyoxypropylene diamine of the type $NH_2CH(CH_3)CH_2[OCH_2CH(CH_3)]_xNH_2$ ($x = 2.6$), which was provided by Huntsman Chemicals under the trade name Jeffamine D230. Jeffamine D2000 (MW ∼2000, $x = 33.1$) was used for the preparation of the heterostructured mixed organic−inorganic ion clay films, as described below. All other chemicals were purchased from Aldrich Chemical Co. and used without further purification.

Preparation of Homoionic and Mixed-Ion Clay Fabric Films. Na^+−montmorillonite (grade PGW, Nanocor Inc.) with a cation-exchange capacity (CEC) of 120 meq/100 g was used for the preparation of homoionic sodium−montmorillonite clay films. A synthetic Li^+−fluorohectorite clay (FH, Corning Inc.) with a CEC similar to that of the PGW montmorillonite was used for the preparation of homoionic lithium−fluorohectorite clay fabric films.

Self-supporting Na^+−montomorillonite and Li^+−fluorohectorite fabric films were prepared by evaporating a 2.5−5.0 wt % aqueous suspension of the clay on a flat surface at room temperature. Depending on the clay content of the suspension, the thickness of the film was 30−60 μm.

Heterostructured mixed organic−inorganic ion clay films were prepared by partial ion exchange of Na^+− or Li^+−clay films with protonated Jeffamine D2000 diamine in ethanol (0.030 M). The contact time for ion exchange was varied from 5 min to 6 h. The washed clay films were dried in air at room temperature for 5 days before use in forming composite films.

Preparation of Epoxy−Clay Fabric Film Composites and Epoxy−Clay Nanocomposites. Pristine glassy epoxy polymer specimens (disks) were prepared by mixing the epoxy monomer (EPON 826) with the curing agent (Jeffamine D230) at 50 °C for ∼30 min; liquid mixture was then outgassed at room temperature and cured on an aluminum disk mold by using an appropriate relief coat at 75 °C for 3 h and at 125°C for an additional 3 h under nitrogen. The formed epoxy disks were polished to an average thickness of ∼0.2 mm (∼8 mL).

For the preparation of the epoxy−clay composite film specimens, the self-supported clay fabric films were dip-coated with a stoichiometric mixture of outgassed EPON 826 and Jeffamine diamine D230 and then cured to form flexible epoxy−clay composite films. The wetted film was suspended vertically to remove excess uncured resin. After being aged 1 day in air, the partially cured composite was heated in an oven at 60 °C for 3 h and then at 125 °C for 3 h in a nitrogen atmosphere to complete the cure.

Thin-disk specimens of epoxy−clay nanocomposite containing randomly oriented clay particles were prepared for comparison purposes by mixing homoionic organoclays or mixed organic−inorganic ion clays with the EPON 826 epoxy precursor and the curing agent diamine D230 and curing the mixture in aluminum disk molds.[36,37]

On the basis of the weight, thickness, and lateral dimensions of a Na^+−montmorillonite film prepared from a 3% (w/v) clay suspension, we found the bulk density of the film to be 2.0 g/cm^3. The specific density of Na^+−montmorillonite platelets is taken to be 2.6 g/cm^3. [38]

Characterization and Testing of Clay Fabric Films and Epoxy−Clay Composites. X-ray diffraction (XRD) patterns were obtained on a Rigaku rotaflex 200B diffractometer equipped with

(21) Usuki, A.; Kawasumi, M.; Kojima, Y.; Okada, A.; Kurauchi, T.; Kamigaito, O. *J. Mater. Res.* **1993**, *8*, 1174.
(22) Usuki, A.; Kojima, Y.; Kawasumi, M.; Okada, A.; Fukushima, Y.; Kurauchi, T.; Kamigaito, O. *J. Mater. Res.* **1993**, *8*, 1179.
(23) Kojima, Y.; Usuki, A.; Kawasumi, M.; Okada, A.; Fukushima, Y.; Kurauchi, T.; Kamigaito, O. *J. Mater. Res.* **1993**, *8*, 1185.
(24) Beall, G. W. In *Polymer−Clay Nanocomposites*; Pinnavaia, T. J., Beall, G. W., Eds.; John Wiley & Sons: New York, 2000; p 267.
(25) Messersmith, P. B.; Giannelis, E. P. *J. Polym. Sci., Part A: Polym. Chem.* **1995**, *33*, 1047.
(26) Kojima, Y.; Fukumori, K.; Usuki, A.; Okada, A.; Kurauchi, T. *J. Mater. Sci. Lett.* **1993**, *12*, 889.
(27) Yano, K.; Usuki, A.; Okada, A. *J. Polym. Sci., Part A: Polym. Chem.* **1997**, *35*, 2289.
(28) LeBaron, P. C.; Pinnavaia, T. J. *Chem. Mater.* **2001**, *13*, 3760.
(29) Chang, J.-H.; Park, K. M.; Cho, D.; Yang, H. S.; Ihn, K. J. *Polym. Eng. Sci.* **2001**, *41*, 1514.
(30) Yeh, J. M.; Liou, S. J.; Lai, C. Y.; Wu, P. C. *Chem. Mater.* **2001**, *13*, 1131.
(31) Xu, R.; Manias, E.; Snyder, A. J.; Runt, J. *Macromolecules* **2001**, *34*, 337.
(32) Strawhecker, K. E.; Manias, E. *Chem. Mater.* **2000**, *12*, 2943.
(33) Wang, Z.; Pinnavaia, T. J. *Chem. Mater.* **1998**, *10*, 3769.
(34) Lan, T.; Kaviratna, P. D.; Pinnavaia, T. J. *Chem. Mater.* **1994**, *6*, 573.
(35) Chaiko, D. J.; Leyva, A. A. *Chem. Mater.* **2005**, *17*, 13.
(36) Triantafillidis, C. S.; LeBaron, P. C.; Pinnavaia, T. J. *J. Solid State Chem.* **2002**, *167*, 354.
(37) Triantafillidis, C. S.; LeBaron, P. C.; Pinnavaia, T. J. *Chem. Mater.* **2002**, *14*, 4088.

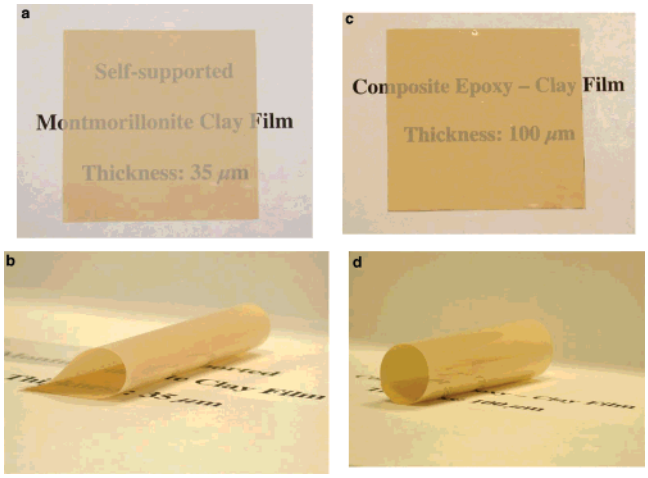

Figure 1. Optical images of (a and b) homoionic inorganic Na^+−montmorillonite clay fabric film with a thickness of 35 μm and (c and d) epoxy−clay fabric film composite with a thickness of 100 μm prepared from the Na^+−montmorillonite clay fabric film.

Cu Kα X-ray radiation and a curved crystal graphite monochromator, operating at 45 kV and 100 mA. Thermogravimetric analyses (TGA) of the clay films were performed using a Cahn TG System 121 Analyzer. The clay films were ground to produce powdered clays, which were heated to 800 °C at a rate of 5 °C/min under a N_2 flow. The compositions of the clay films were determined by energy dispersive spectroscopy (EDS), CHN chemical analysis, and thermal gravimetric analysis (TGA). Dynamic mechanical analysis (DMA) tests were performed on a 2980 dynamic mechanic analyzer (TA Instruments) in the three-point bending mode at a frequency of 1 Hz and amplitude of 20 μm over the temperature range 25−140 °C. The heating rate was 4 °C/min. The pristine epoxy polymer and the epoxy−clay film composite specimens were rectangular bars with dimensions 60 mm × 13 mm × 3 mm. The latter were prepared by encapsulating a clay film in a 3 mm thick epoxy specimen before final curing of the composite. Oxygen permeability measurements were performed on a Mocon Ox-tran 2/60 oxygen permeability instrument with 100% oxygen as test gas. The specimens tested were the pristine epoxy polymer disks and the epoxy−clay nanocomposite disks with an average thickness of ∼0.2 mm (∼8 mL), and the epoxy−clay fabric film composites with an average thickness of ∼0.10−0.15 mm.

Results and Discussion

Composition and Structural Properties of Clay Fabric Films. The formation of self-supporting clay fabric films depends on the ability of the clay particles to form colloidal clay−water suspensions with a high degree of nanolayer exfoliation. Upon the evaporation of the suspensions on a flat surface, the platelets align and overlap to form opaque (Li^+−fluorohectorite) and semitransparent (Na^+−montmorillonite) films. Optical images of a Na^+−montmorillonite film (PGW) with a thickness of 35 μm are shown in images a and b of Figure 1. The light brown clay film is smooth, continuous, flexible, and semitransparent.

Epoxy−clay fabric film composites were prepared by impregnating the clay film with a stoichiometric mixture of the epoxy resin and the Jeffamine diamine curing agent D230 and then curing the mixture at 125 °C. As shown by optical images c and d in Figure, the composite films made from Na^+−montmorillonite retain the monolithic properties of the initial film. Equivalent mixed organic−inorganic ion clay fabric film composites were obtained by first modifying the clay film through partial ion exchange of the Na^+ ions (or Li^+ in the case of flurohectorite) at the outer regions of the film with protonated Jeffamine diamine D2000 ions, denoted $D2000^+$.

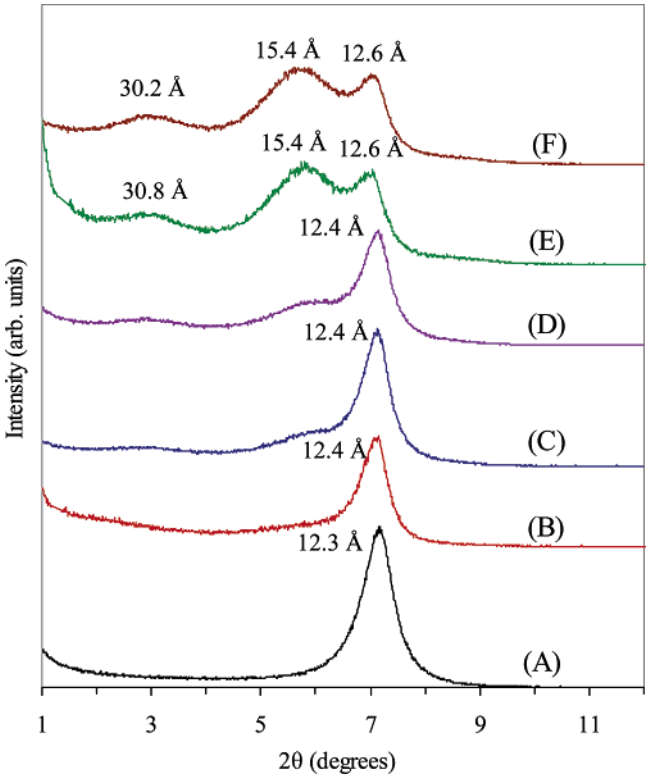

Figure 2. X-ray diffraction (XRD) patterns of (A) homoionic Na^+−montmorillonite clay film and the heterostructured mixed Na^+−$D2000^+$ ion-exchanged montmorillonite clay films formed after reaction times in ethanolic 0.03 M protonated D2000 of (B) 5 min, (C) 30 min, (D) 2 h, (E) 6 h, and (F) 6 h. All mixed-ion films were washed with ethanol after ion exchange, except the film shown in part E.

The XRD patterns of a Na^+−montmorillonite film after ion-exchange reaction with protonated $D2000^+$ diamine cations for different reaction times are shown in Figure 2. Figure 3 shows the corresponding patterns for a similar set of Li^+−fluorohectorite film samples. From the XRD patterns, it can be seen that there is a gradual replacement of the inorganic cations by the organic $D2000^+$ cations at the outer regions of the film that results in the expansion of the clay basal from ∼12.5 Å for the inorganic clay to ∼30 Å for montmorillonite and ∼53 Å for fluorohectorite. The expansion in basal spacings is consistent with the intercalation of the organic cation between some, but not all, clay layers. A significant fraction of the initial inorganic phase with a spacing of ∼12.5 Å remains after reaction times of 6 h and 30 min for montmorillonite and fluorohectorite, respectively. The faster ion-exchange kinetics for the Li^+−fluorohectorite can be attributed to the higher charge-to-radius ratio of the smaller initial exchange cation (Li^+), which facilitates solvation and osmotic swelling of the interlayers by the ethanol solvent.

The powdered forms of Na^+−montmorillonite and Li^+−fluorohectorite undergo complete ion exchange with $D2000^+$ cations after reaction times of 6 h and 30 min, respectively. Thus, it is clear from the XRD patterns for the clay films that the replacement of the inorganic by organic cations

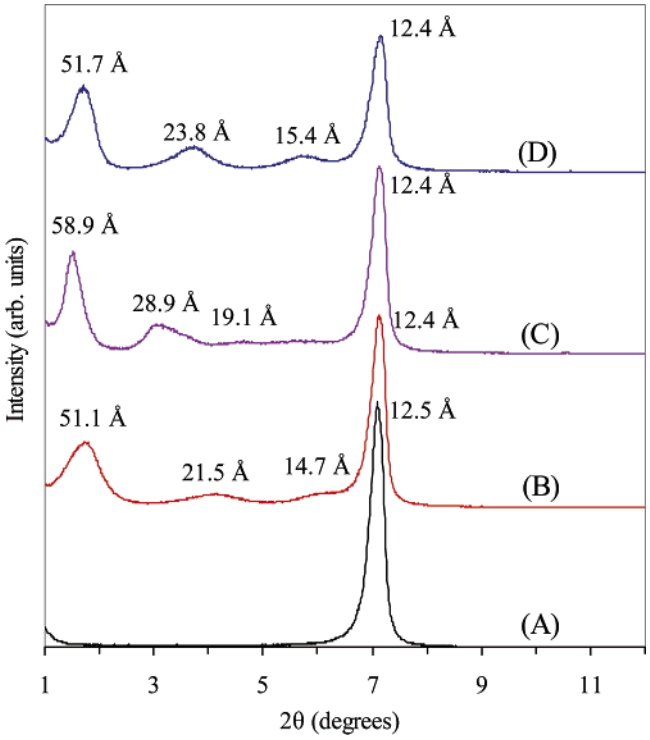

Figure 3. X-ray diffraction (XRD) patterns of (A) homoionic Li^+−fluorohectorite clay film and of the heterostructured mixed Li^+−$D2000^+$ ion-exchanged films after reaction times in ethanolic 0.03 M protonated D2000 of (B) 5, (C) 30, and (D) 30 min. All mixed-ion films were washed with ethanol after ion exchange, except for the film shown in part C.

occurs starting from the outer surfaces of the films and proceeds inward. As is illustrated schematically in Figure 4, this diffusion-limited exchange process results in a heterostructured mixed-ion monolith, wherein organic cations occupy exchange sites on clay platelets at the external surfaces of the film, inorganic cations occupy exchange sites on the interior clay platelets, and a mixture of inorganic and organic cations on the platelets are located between these two homoionic clay phases.

The heterostructured nature of the mixed-ion clay films is verified by chemical analysis using TGA, CHN, and SEM-EDS methods. The TGA curves for the montmorillonite films in Figure 5 show that increasing the ion-exchange reaction times increases the $D2000^+$ content of the clay film. The TGA curves for the fluorohectorite mixed-ion films (not shown) were similar to those for montmorillonite, differing only in a relatively higher $D2000^+$ loading. Table 1 compares the bulk compositions of montmorillonite and fluorohectorite films determined by elemental CHN analysis with the compositions found by the surface-selective SEM-EDS method. The SEM-EDS results show there are far more $D2000^+$ cations at the surface of the film than is indicated by bulk chemical analysis.

Barrier Properties of Epoxy−Clay Fabric Film Composites. Our clay fabric film approach to barrier composite formation provides an exceptionally high degree of clay platelet alignment, as well as a very high volume-filling fraction of platelets. The bulk density of a pristine Na^+−montmorillonite film (2.0 g/cm^3) is smaller than the specific density of a clay nanolayer (2.6 g/cm^3),[38] indicating that approximately 23 vol % of the film is unoccupied by clay

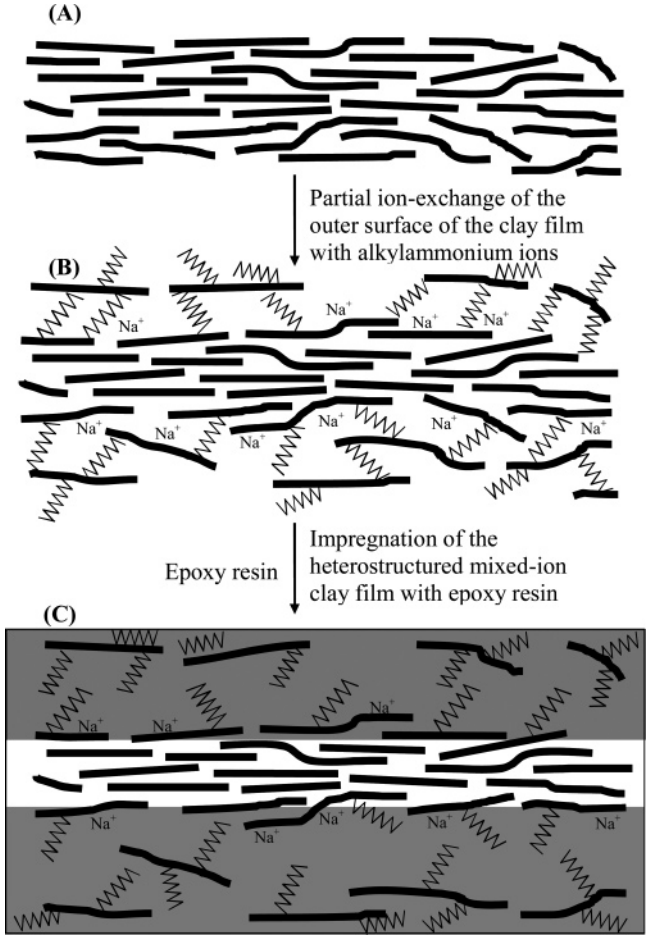

Figure 4. Schematic representation of the structure of (A) homoionic Na^+−montmorillonite clay fabric film (Na^+ ions not shown), (B) a heterostructured mixed-ion Na^+−$D2000^+$ montmorillonite clay fabric film with fully exchanged platelets on the outer surfaces of the film and a central phase of Na^+−montmorillonite, and (C) a cured epoxy−clay fabric film composite with exfoliated clay nanolayers at the outer surfaces of the clay film.

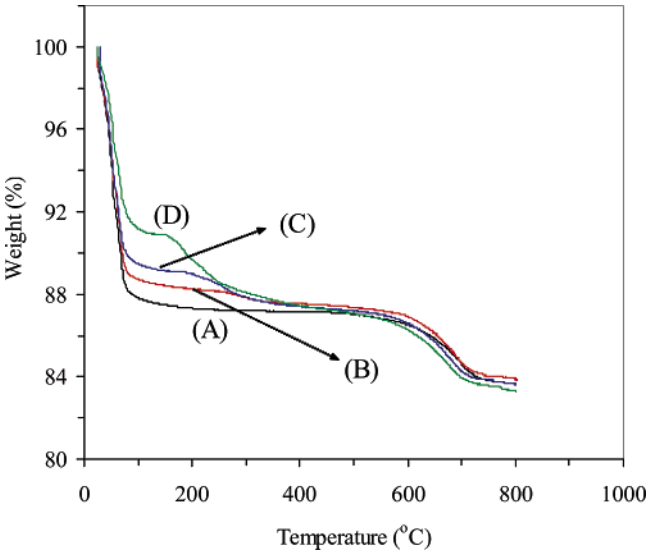

Figure 5. Thermogravimetric analysis (TGA) curves for (A) homoionic Na^+−montmorillonite clay film and heterostructured Na^+−$D2000^+$ mixed-ion exchanged montmorillonite clay films formed after reaction times of (B) 30 min, (C) 2 h, and (D) 6 h. All mixed-ion films were washed with ethanol after ion exchange.

nanolayers. The high oxygen permeability of a pristine Na^+−montmorillonite film (>6000 cm^3 mL/m^2 day) is consistent with the presence of a substantial void volume within the

Table 1. Compositions of Heterostructured Mixed Organic−Inorganic Ion Clay Fabric Films as Determined by Elemental CHN and SEM-EDS Analysis

sample[a]	time for $D2000^+$ exchange	% $D2000^+$ exchange CHN	% $D2000^+$ exchange EDS
Na^+, $D2000^+$−montmorillonite	5 min	0.8	28
	30 min	1.6	38
	2 h	2.8	50
	6 h	3.5	62
Li^+, $D2000^+$ −fluorohectorite	5 min	4.7	
	30 min	8.0	

[a] Each sample was washed free of excess $D2000^+$ salt prior to analysis

film. Upon impregnating the fabric film with epoxy polymer, however, we find that the oxygen permeabilities of the resulting composites are 2−3 orders of magnitude lower than that of the pristine epoxy polymer and 3−4 orders of magnitude lower than that of the pristine clay films. Reductions of this magnitude are unprecedented among all known epoxy composites. We observed reductions in oxygen permeabilities of only 5−20% when Na^+-, Li^+-, and $D2000^+$-exchanged montmorillonite clays are dispersed according to previously described methods[37] in an EPON 826-D230 epoxy polymer at the 6 wt % level on a silicate basis. Recent advances[39] in the use of magnetic fields to align smectite clay layers in epoxy polymers promise to improve the barrier properties of the composites, but platelet alignments comparable to a clay fabric film are unlikely.

As shown by the oxygen permeability values in Table 2, the reductions in permeability obtained for the clay composite films are independent of both the width-to-thickness aspect ratio of the clay (∼200 for montmorillonite vs ∼2000 for fluorohectorite) and the nature of the exchange cation at the external surfaces of the film.The barrier properties of polymer−clay nanocomposites normally are described in terms of the Nielson[40] tortuous path model or, more preferably, a refined version of that model.[41,42] The clay fabric film structure responsible for the barrier properties observed in the present work is not expected to conform to the tortuous path model. In the case of Na^+ and Li^+ clay films, there is little or no intercalation of polymer between the basal planes of the clay platelets, because the basal spacing does not change upon polymer impregnation into the film. As is illustrated in Figure 6, the 23% void volume of a Na^+−montmorillonite fabric film most likely arises from the imperfect tiling of the clay during film formation. The voids between the clay edges represent the volume that is filled upon polymer impregnation of the film. Experimentally, we find the thickness of a cured epoxy−Na^+−montmorillonite composite film to be consistent with the penetration of the polymer into essentially all of the available free volume in the film.

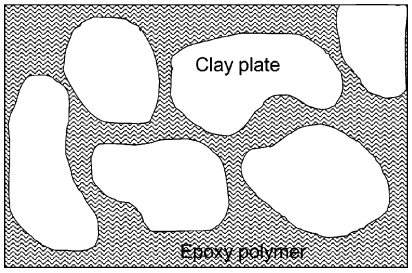

Figure 6. Schematic illustration of polymer filling voids between clay platelet edges in an epoxy−inorganic clay fabric film composite. The view is orthogonal to the oriented clay nanolayers.

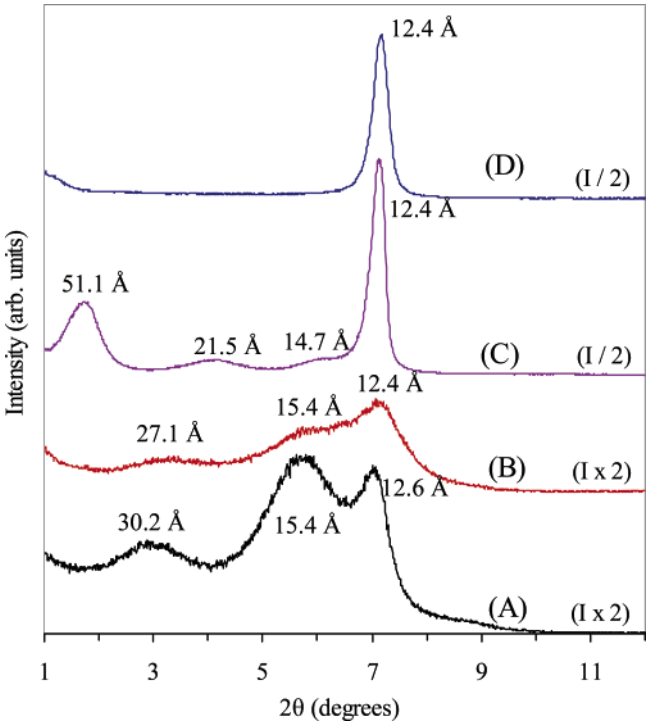

Figure 7. X-ray diffraction (XRD) patterns of (A) a heterostructured Na^+−$D2000^+$ mixed-ion montmorillonite clay film, (B) epoxy−clay composite film prepared from the clay film in part A, (C) a heterostructured Li^+−$D2000^+$ mixed-ion fluorohectorite clay film, and (D) epoxy−clay composite film prepared from the clay film in part C.

In the case of the heterostructured mixed ion Na^+−$D2000^+$ and Li^+−$D2000^+$ clay films, there is some intercalation and exfoliation of the clay platelets at the $D2000^+$-rich platelets at the outer regions of the fabric film. As shown by the comparisons of diffraction patterns in Figure 7, evidence for clay layer swelling by polymer in the mixed-ion films is provided by the decreases in the relative intensities for the diffraction peaks characteristic of the organoclay fraction of the film. However, the basal spacings for the inorganic clay fraction at the centers of these films do not undergo an expansion in basal spacing upon polymer composite formation. Thus, the interior regions of the mixed-ion films share

Table 2. Oxygen Permeability Data for Epoxy−Clay Fabric Film Composites

clay fabric film composition	thickness of clay fabric film (mm)	thickness of epoxy−clay fabric film composite (mm)	oxygen permeability ((cc mL)/(m^2 day))
pristine epoxy		0.20	98.9
Na^+−montmorillonite	0.060	0.11	≤0.1
Na^+−montmorillonite	0.035	0.10	0.97
Li^+−fluorohectorite	0.065	0.14	1.2
Na^+−$D2000^+$ montmorillonite	0.060	0.12	0.28
Li^+−$D2000^+$ fluorohectorite	0.065	0.14	≤0.1

the same nonswelling fabric structure and same barrier mechanism as an inorganic clay film composite.

We do not expect the exceptionally high barrier properties of clay fabric film nanocomposites to conform to the parallel plate or torturous path model of Neilson.[40] Although the clay platelets are aligned parallel to each other in the fabric film, an insignificant fraction of the polymer occupies space between the clay platelets, as evidenced by the absence of an expanded basal spacing for Na^+−montmorillonite and Li^+−fluorohectorite upon impregnation of the film by polymer. Also, the central inorganic phase of the hetero-structured mixed organic−inorganic ion films do not undergo swelling upon polymer formation. Instead, the high barrier properties of clay fabric films most likely arise from the filling of voids between platelet edges, as described in Figure 6. In this case, the more appropriate barrier nanocomposite model may be the one proposed by Beall,[24] wherein the polymer at the interface of the particle filler plays a dominant role in determining the barrier properties of the composite.

Mechanical Properties of Epoxy−Clay Fabric Film Composites. Mechanical testing data were obtained using the DMA three-point bending method and 3 mm thick epoxy-clay fabric film composite specimens. Regardless of the composition of the clay fabric film, each specimen exhibited a storage modulus equal to or slightly larger than the modulus of the pristine epoxy polymer (e.g., ∼2.8 GPa at 40 °C). In addition, the glass-transition temperatures of the epoxy−clay film composites, which were determined from the maximum in the tan δ vs temperature curves, was higher by 2−4 °C compared to the T_g of the pristine polymer (∼84 °C). Thus, clay fabric film composites do not compromise the mechanical properties of the polymer.

Acknowledgment. This work has been supported by the NASA John Glenn Research Laboratory and the MSU Composite Materials and Structure Center.

CM060825T

(38) Osman, M. A.; Mittal, V.; Lusti, H. R. *Macromol. Rapid Commun.* **2004,** *25,* 1145.
(39) Koerner, H.; Hampton, E.; Dean, D.; Turgut, Z.; Drummy, L.; Mirau, P.; Vaia, R. *Chem. Mater.* **2005**, *17,* 1990.
(40) Neilson, L. E. *J. Macromol. Sci., Chem.* **1967**, *A1* (5), 929.
(41) Fredrickson; G. H.; Bicerano, J. *J. Chem. Phys.* **1999**, *110,* 2181.
(42) Cussler, E. L.; Hughes, S. E.; Ward, W. J., III; Aris, R. *J. Membr. Sci.* **1988**, *38,* 161.